













In search of universalities in the dissociative photoionization of PANHs via isomerizations

Arun S,¹  Karthick Ramanathan,¹  Muthuamirthambal Selvaraj,¹  Marco Cautero,^{2,a)} 
Robert Richter,²  Nitish Pal,²  Jacopo Chiarinelli,³  Paola Bolognesi,³  Lorenzo Avaldi,³ 
M. V. Vinitha,¹  Chinmai Sai Jureddy,¹  and Umesh R. Kadhane^{1,b)} 

AFFILIATIONS

¹ Indian Institute of Space Science and Technology, Thiruvananthapuram 695547, Kerala, India

² Elettra-Sincrotrone Trieste, Strada Statale 14 - km 163, 5 in AREA Science Park, Basovizza, TS 34149, Italy

³ CNR-Istituto di Struttura della Materia, Area della Ricerca di Roma 1, Monterotondo, Roma 00015, Italy

^{a)} Also at: Dipartimento di Ingegneria e Architettura, University of Trieste, Trieste 34127, Italy.

^{b)} Author to whom correspondence should be addressed: umeshk@iist.ac.in

ABSTRACT

In search of the cause behind the similarities often seen in the fragmentation of PANHs, vacuum ultraviolet (VUV) photodissociation of two pairs of isomers quinoline–isoquinoline and 2-naphthylamine-3-methyl-quinoline are studied using the velocity map imaging technique. The internal energy dependence of all primary fragmentation channels is obtained for all four target molecules. The decay dynamics of the four molecules is studied by comparing their various experimental signatures. The dominant channel for the first pair of isomers is found to be hydrogen cyanide (HCN) neutral loss, while the second pair of isomers lose HCNH neutral as its dominant channel. Despite this difference in their primary decay products and the differences in the structures of the four targets, various similarities in their experimental signatures are found, which could be explained by isomerization mechanisms to common structures. The fundamental role of these isomerization in controlling different dissociative channels is explored via a detailed analysis of the experimental photoelectron–photoion coincidences and the investigation of the theoretical potential energy surface. These results add to the notion of a universal PANH fragmentation mechanism and suggests the seven member isomerization as a key candidate for this universal mechanism. The balance between isomerization, dissociation, and other key mechanistic processes in the reaction pathways, such as hydrogen migrations, is also highlighted for the four molecules.

I. INTRODUCTION

Polycyclic aromatic hydrocarbons (PAHs) and their nitrogenated counterparts, PANHs are a class of organic molecules that are of great interest to different fields, such as environmental chemistry,¹ combustion chemistry,^{2,3} and molecular astrophysics.^{4,5} In the astronomical context, they are hypothesized to be carriers of the diffuse interstellar bands^{6,7} and thus are strongly suggested to be ubiquitous in the interstellar medium. Spectroscopic evidence from space missions, such as Cassini, also point to them being present in different planetary media, such as Titan,⁸ and Iapetus and Phoebe.⁹ Furthermore, recent studies¹⁰ have directly identified individual members of the PA(N)H family in photo-active media, such as the TMC molecular cloud. The ubiquity of these molecules and their strong well characterized features make them useful candidates

for tracers in different astronomical media, such as star-forming regions.¹¹

These molecules are also thought to play a very important role in influencing the local chemistry and contributing to the inventory of organic molecules in different regions of the universe. For instance, it is hypothesized that PAHs are responsible for the formation of fullerenes^{12–14} in space like conditions. Laboratory studies¹⁵ have also indicated that, via hydrogenation and hydroxylation reactions, they can be transformed into more complex molecules, even at temperatures as low as 5 K, typical of dense molecular clouds. Apart from these associative pathways, their dissociative chemistry in response to different radiation conditions is also suggested to be an important source of smaller hydrocarbons and other reactive fragments in different astronomical media.^{16,17} The fragments produced as a result of this “top-down” model are also important



FIG. 1. Targets studied: (a) isoquinoline, (b) quinoline, (c) 2-naphthylamine, and (d) 3-methyl-quinoline.

in their own regard. One of such important fragments is hydrogen cyanide (HCN), known to be one of the dominant neutrals products in the dissociation of many different PANHs.^{18,19} Adenine, one of the four nucleobases in DNA, is a pentamer of HCN, and various studies^{20,21} have established the importance of HCN in adenine's formation even in environments analogous to extremely cold interstellar clouds.²² Another interesting example is hydrogen iso-cyanide (HNC), which is also produced as a dominant neutral product²³ in dissociative processes. HNC is known to be highly reactive and would rapidly isomerize to HCN under suitable conditions.^{24–26} Its detection in the interstellar medium²⁷ in large quantities prompts the question of their production mechanism given its rapid isomerization to HCN in the presence of solid interfaces (grains, dust). Similarly, other astronomically relevant molecules, such as members of the cyanopolyne family, have also been detected^{19,28} as fragments from the dissociation of PANHs. Hence, a detailed study of the dissociative processing of PANHs and the formed products would provide great insights into their role in chemical evolution in space.

In this context, structural rearrangements or isomerization prior to dissociation is an important process that deserves more attention. Multiple studies have found great similarities in the experimental spectra of different PA(N)Hs with varying structures, indicative of a common mechanism underneath.^{29,30} Isomerization mechanisms that bring different isomers to common ground before further dissociation is a plausible explanation behind these observations. For instance, it was shown both theoretically and experimentally that naphthalene prefers to isomerize to azulene prior to C_2H_2 abstraction.^{31,32} A similar observation has been reported in the case of quinoline, a nitrogenated analog of naphthalene^{19,33} for the cases of HCN and C_2H_2 abstractions. This was also extended to larger ring structures;³⁴ for instance, acridine and phenanthridine were shown to preferentially isomerize to common structures before further dissociation.³⁵ Even in processes that appear relatively simple like neutral hydrogen losses, where at first glance, one might expect that only direct bond fission of the C–H bond to play a role, hydrogen migrations leading to various C–H shifted isomers were found to precede the hydrogen dissociation channels.^{36–38} These isomerization mechanisms have persistently appeared in different theoretical studies too^{39–41} and possibly hint toward a universal behavior⁴² behind the dissociation of this family of PA(N)Hs. However, the dynamical details of these mechanisms are not directly decipherable from most experimental spectra. Even in theoretical studies, not every mechanism predicted is reflected in reality. It is only with a combined theoretical and experimental investigation, backed with comprehensive calculations supported with corroborating experimental signatures that these aspects of the dissociation process can be brought forth.

The present study aims to take a closer look into the isomerizations that play a vital role in the dissociation of different PA(N)Hs. A set of four double ringed heteroaromatic target molecules with different structural attributes (refer to Fig. 1), 2-Naphthylamine (NPA), 3-Methyl-Quinoline (MeQ), Quinoline (Q), and Isoquinoline (IsoQ), were chosen, which would be used as case-studies for isomerization trends. Quinoline and isoquinoline were chosen for the differences in the relative position of the nitrogen in the parent ring. Naphthylamine and methyl-quinoline were chosen to study the role of a substituent in further dissociation. Apart from providing ideal test cases for our study, these targets themselves are of great astronomical interest. Quinoline, isoquinoline, along with two different methyl-quinolines, have been directly identified in Murchison meteorite.^{43,44} Likewise, amino along with cyano-substituted PAHs are proposed to be present on interplanetary dust particles⁴⁵ and comets.⁴⁶ With the increasing number of detection of these smaller organics in different astronomical media, and studies showing that these molecules can survive in these harsh environments for longer periods than previously expected,⁴⁷ investigations into the response of these molecules to radiation conditions akin to space would have direct relevance in the astrochemical community.

Among the dissociation channels of the monocation, the four primary prominent decay channels that are usually observed in the experimental spectra are methyl amidogen HCNH loss, acetylene C_2H_2 loss, hydrogen cyanide HCN loss/hydrogen isocyanide HNC loss, and neutral hydrogen H loss. These are discussed in detail using reaction pathways constructed by electronic structure calculation, which includes some mechanisms that were previously unreported. Relevant details of the potential energy surfaces (PES) of these channels are put forth and their attributes that are backed by experimental observations are highlighted. In this manner, a synergistic theoretical and experimental investigation of their dissociation pathways has allowed the identification of certain commonalities, which may point out some potentially universal features of PANHs subject to extreme radiation conditions in extra-terrestrial environments.

II. EXPERIMENTAL DETAILS

The experiments were performed at the Velocity Map Imaging (VMI) endstation in Elettra-Sinchrone facility (Trieste, Italy). Detailed description of the endstation and the beamline is given elsewhere,⁴⁸ and only a brief summary of the VMI endstation is given here. The endstation consists of a VMI setup equipped with a position sensitive detector (VMI detector) capable of measuring the velocity of the detected particle and a Time-of-Flight (ToF) setup with a microchannel plate detector (ToF detector) that measures the time of flight of the detected particle mounted opposite each other. The setup can be operated in two modes, ion-on-VMI

and electron-on-VMI, depending on the polarity of the voltage settings of the electrodes. The former is used to obtain the kinetic energy release distributions (KERD) of the fragmenting daughter ions, while the latter is used to obtain the photoelectron spectra and the PEPICO spectra from which the branching ratios (BRs) of the different fragmentation channels. All four samples were bought from Sigma-Aldrich and were used without further purification. Due to the low vapor pressure of naphthylamine, additional heating was required to provide sufficient target density in the chamber, while the other three targets were used without any heating. Neon and xenon gasses were used for the calibration of the photoelectron spectra and Time of Flight (ToF).

Photon energies ($h\nu$) ranging from 20 to 36 eV were used in the experiment. All ions that were detected within 9 μ s from the detection of a photoelectron were taken as true events. The maximum ToF recorded in the experiment is 6.4 μ s, corresponding to the ToF of the 143 isomers. Thus, the chosen time window of 9 μ s is enough to capture all daughter ions in the experiment. Events in which only one ion was detected in coincidence with an electron were used to construct the mass spectra with the time of flight of ions computed from the start signal provided by the photoelectron detection. The kinetic energy (KE) of the electrons (or ions) was obtained from their positional information, recorded by the VMI detector. This is done using the MEVELER program, which extracts velocity maps by inverting their positions using maximum entropy reconstruction.⁴⁹ From the velocity maps of the electrons, the binding energy (BE) of the corresponding ions is calculated via the formula $BE = h\nu - KE$ for a given photon energy, $h\nu$, and coincident electron kinetic energy, KE. The photoelectron spectra are obtained by calculating the binding energy from the positions of all electrons detected. The PEPICO spectra and branching ratios of different channels were obtained by calculating the binding energy of electrons detected in coincidence with the ions of the corresponding channel. The flight time of the ions in the two modes is different due to the difference in the length of the drift tubes. The results from the ion-on-VMI mode are used for any spectra comparison due to its better mass resolution as a result of its longer drift tube.

III. COMPUTATIONAL DETAILS

Reaction mechanisms are computed for the loss of C_2H_2 , HCN, HNC, and HCNH in quinoline, naphthylamine, methyl-quinolone, and isoquinoline mono-cations depending on whether the channel is seen in the experimental spectra. These computations were performed using the GAUSSIAN 09 software.⁵⁰ Potential energy surface scans were performed at the B3LYP/6-311++G(d,p) level of theory in order to locate the structures of the stationary points involved, and the pathways with the lowest energy barrier leading up to each of the structures considered are reported. Geometries were optimized (with transition states optimized using Berny's algorithm) at the same level of theory, and vibrational frequencies were used to characterize the structures as minimas (intermediates) and first-order saddle points (transition states). Intrinsic reaction coordinate (IRC) calculations were carried out in select steps to verify that the corresponding transition state indeed connects the expected local minimas on either side of the reaction coordinate.

All pathways explored and optimized along with their energetics are reported in the supplementary material. Brief summaries

and important attributes in their mechanisms are highlighted in the following sections. A detailed exploration of the dissociating landscape of the quinoline monocation is already reported earlier,³³ and relevant results from the previous work are recalled as and when necessary. Experimental parallels are drawn as the pathways are discussed, and possible explanations are given to explain them.

IV. RESULTS

The results of the four targets would be grouped in two sets. The results of mass 129 isomers (Q and IsoQ) and mass 143 isomers (Npa and MeQ) will be discussed in tandem for the sake of clarity.

A. Mass 129 isomers

The mass spectra of the mass 129 isomers normalized to total yield recorded at 23 eV photon energy are depicted in Fig. 2(a). The major peaks seen in both cases apart from the parent at m/z 129 are the peaks at m/z 128, 103, 102, and 101. Other minor peaks appear at m/z 76, 77, and 78. As can be seen from Fig. 2(a), a great similarity between the two spectra with all the major peaks in isoquinoline being slightly more intense than the corresponding peaks in quinoline (except in the case of the peak at m/z 76, where the order reverses but only with a minor difference again) is seen. This minor difference in their relative intensities could be due to the difference in their ionization energies, which are about 0.1 eV apart;¹⁸ hence, it is most likely that the dissociative channels in isoquinoline open at a lower energy than in quinoline and thus dissociate a little more profusely. Otherwise, their mass spectra look nearly identical in terms of not only their major channels but also in their relative yields. This similarity will be used to assign the channels to the peaks based on the previous work on quinoline.¹⁹

For both molecules, the peak at m/z 128 can be unambiguously attributed to the loss of neutral hydrogen from the parent. The peak at m/z 103 is assigned to the loss of neutral acetylene, while the peak at m/z 102 is assigned to the loss of either hydrogen cyanide or hydrogen isocyanide neutral loss. The peak at m/z 101 could be due to the loss of the methyl amidogen neutral radical or could be due to the sequential loss of hydrogen and one of the mass 27 isomers. In the case of quinoline, the peak at m/z 101 was assigned to the sequential loss of hydrogen followed by hydrogen cyanide.¹⁹ Based on the similarity between the two mass spectral features and for reasons that will be explained shortly after, the peak at m/z 101 in isoquinoline is also assigned to be that of a sequential loss of hydrogen and hydrogen cyanide. In the case of quinoline, the peak at m/z 78 was assigned to the loss of neutral HC_3N producing benzene, and the peaks at m/z 76 and 77 are due to sequential losses of HCN and C_2H_2 (for the m/z 76 peak) and two C_2H_2 losses (for the m/z 77 peak). Again due to the similarity between the mass spectra, these assignments are suggested to hold true for isoquinoline too.

In order to obtain the internal energy dependence of the various dissociative channels, the electron-on-VMI mode is used. In this mode, two factors affect the mass resolution, one is the shorter drift tube, which affects all peaks, while the other is the kinetic energy release, which depends on the dissociation channel. Due to this, while the parent and the hydrogen loss channels are resolved in the mass spectra, the peaks at m/z 101, 102, and 103 are not. This could be because the hydrogen loss channel is known to be barrierless,

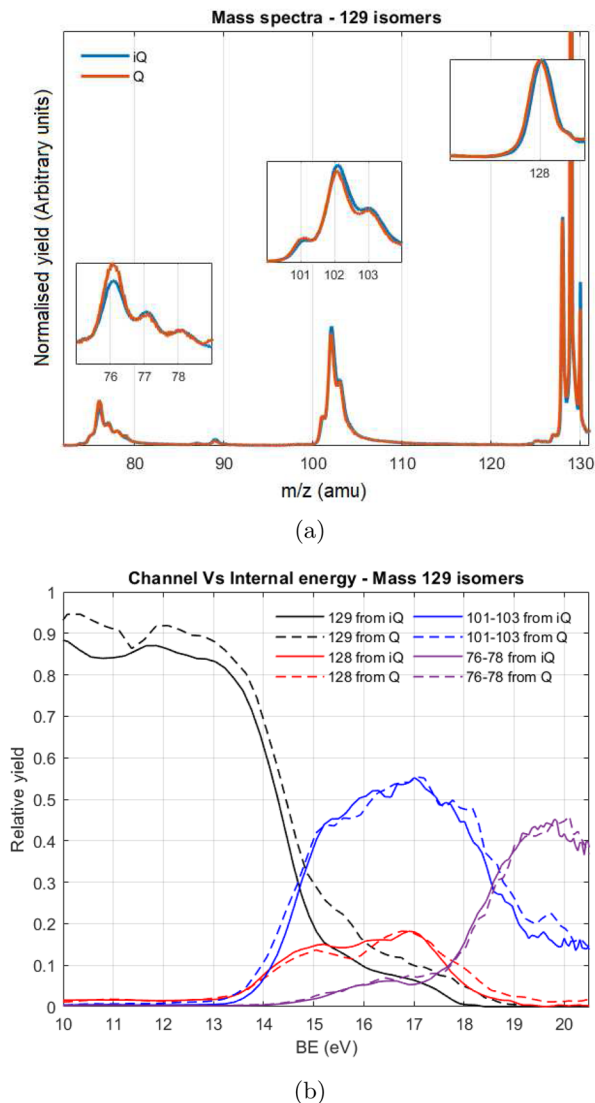


FIG. 2. (a) Mass spectra at 23 eV photon energy and (b) branching ratios as a function of the binding energy in Q+ and IsoQ+.

while the HCN and C_2H_2 loss channels might possess a reverse barrier³³ and have considerable kinetic energy release. Hence, at first, the entire region covering the peaks of m/z 101, 102, and 103 is taken as one and the corresponding branching ratio is obtained. The other regions taken into considerations is the parent peak, the hydrogen loss peak, and the family of unresolved peaks at m/z 76-78. The obtained branching ratios are then normalized to the total photoelectron spectra and are depicted in Fig. 2(b).

The main feature in both the molecules is their remarkable resemblance to each other. This strongly suggests that the dynamics followed by quinoline is closely followed by isoquinoline too. From the previous work on quinoline,¹⁹ among the m/z 101-103 peaks, 102(12.5 eV BE) opens first, followed by 103(13.3 eV BE) with 101(16.5 eV BE) opening significantly later with the hydrogen loss

peak opening along with 102 at 12.5 eV BE. The current experiment is characterized by larger kinetic shift due to shorter flight times, and hence the first channels open up only at 13.8 eV. In the current scenario, the hydrogen loss channel and the m/z 101-103 region open together at 13.8 eV. This could be due to the 102 channel's contribution to the m/z 101-103 region, which is known to open with the hydrogen loss channel. The m/z 76-78 curve has its onset at 14.5 eV and rapidly starts increasing after 17 eV. This behavior again agrees well with the previous results,¹⁹ wherein the peak at m/z 78 due to a single loss of HC_3N opens early at 13.3 eV with the lowest intensity among the four primary channels. Considering this, the initial portion of the m/z 76-78 curve with its reduced intensity may be the contributions from the m/z 78 peak, while the later part rising beyond 17 eV contains the contributions from the sequential loss channels at m/z 76 and m/z 77. Beyond 18 eV, as the m/z 76-78 curve picks up in intensity, the m/z 101-103 curve falls. This portion of the 101-103 curve beyond 18 eV points to contributions from the m/z 101 peak, which we then re-affirm to be a sequential loss channel. Considering that the sequence responsible for the m/z 101 peak was due to loss of hydrogen and hydrogen cyanide in quinoline and by the match in the features of the branching ratios, the same should hold true for isoquinoline too. The branching ratios that are further mass selected are compared to qualitatively discern the contributions from the different channels. Further details and results are reported in the accompanying supplementary material.

From the observed similarities between the features of both the mass spectra and branching ratios of the two molecules, it is clear that both molecules follow similar decay dynamics. However, there exists a key structural difference between the two molecules due to the relative position of the nitrogen with respect to the carbon in the parent ring. This is reflected computationally in the dissociative pathways computed earlier¹⁸ wherein the energetics of isoquinoline's pathways, while not drastically different, lie below the corresponding pathways in quinoline. Considering the near exact match of their experimental signatures, the most probable explanation behind these strikingly similar features could in fact be isomerization, wherein both molecules isomerize to common structures before they dissociate further. In the case of quinoline, the monocation was predicted to isomerize prior to dissociation.³³ It would be shown computationally in later sections that isoquinoline not only possess isomerization channels, but it also has access to the very same isomers as quinoline, and hence it is not unreasonable to accept that both molecules isomerize to common isomers before dissociation. Another proof comes when the position coordinates of the ions (recorded in *i*-VMI mode) from the $m/z = 102$ (and $m/z = 103$) peak from the two molecules are compared as reported in the supplementary material. These ion images of the two molecules match remarkably well, indicating that both molecules would have fragmented from a common structure, which is well in line with the observations so far.

B. Mass 143 isomers

The mass spectra recorded at $h\nu = 23$ photon energy of the mass 143 isomers are depicted in Fig. 3(a). In the case of methylquinoline, there are two main fragments that dominate the spectra, one at m/z 142 and another at m/z 115, whereas in the case of naphthylamine, the peak at m/z 142 is absent. The peak at m/z 142 can

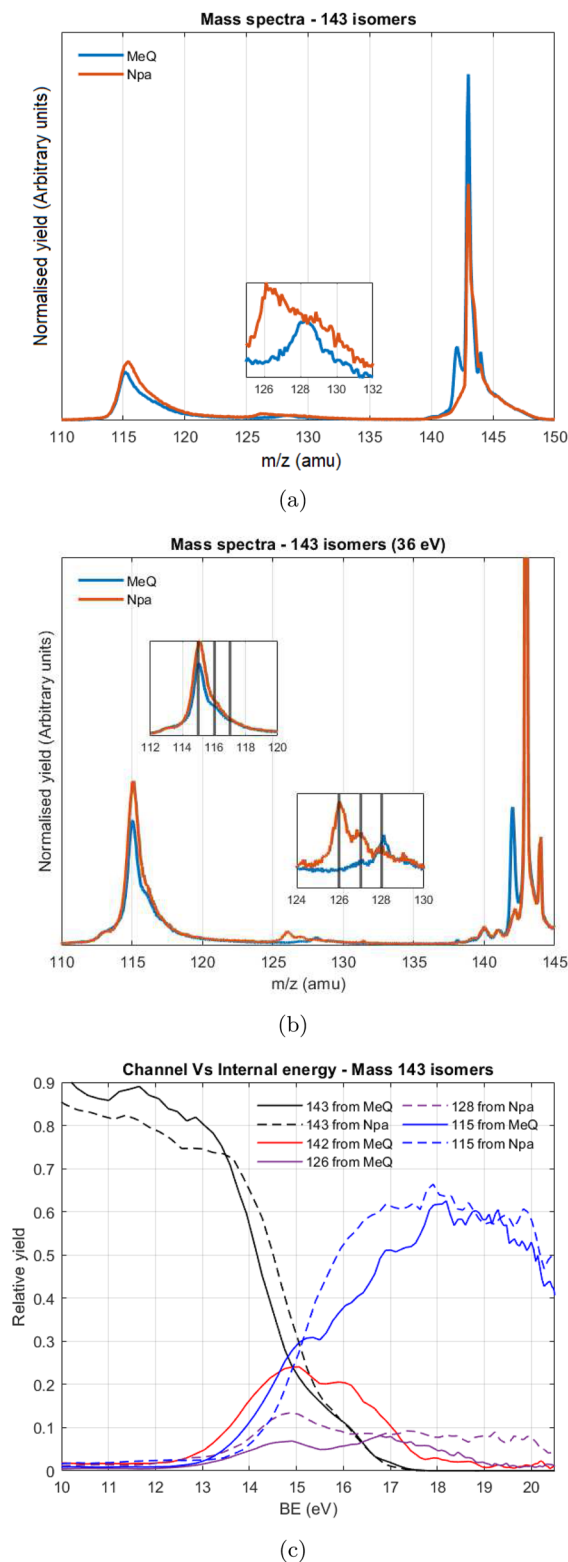


FIG. 3. Mass spectra at (a) 23 eV, (b) 36 eV photon energy, and (c) branching ratios as a function of the binding energy in MeQ⁺ and Npa⁺.

be unambiguously assigned to the loss of neutral hydrogen from the parent, present in large quantities for methyl-quinoline but is negligible in the case of naphthylamine. This difference in the hydrogen loss channels is further elaborated upon in later sections. For both targets, the peak at m/z 115 exhibits a broad peak along with a long tail. The broad extent of this peak is due to a combination of the metastable nature of the decay and kinetic energy release accompanying the ionic fragment, and due to this, it is not possible to extract quantitatively the contributions from the neighboring m/z 116 peak. The two peaks do not get resolved at higher photon energies too; however, the m/z 115 peak shrinks in width, revealing a shoulder like feature at higher energies, which does indicate that there exists a small contribution from the m/z 116 peak as shown in Fig. 3(b). This minor channel is assigned to the loss of either hydrogen cyanide HCN or hydrogen isocyanide HNC. There are three plausible channels that may contribute to the dominant peak at m/z 115 due to the loss of 28 amu neutral fragment, namely, the loss of the methyl amidogen neutral (HCNH) or the sequential loss of hydrogen and HCN\HNC or vice versa. All three possibilities could be applicable in the case of methyl-quinoline; however, considering the absence of the hydrogen loss channel in naphthylamine, it is not very plausible that the m/z 115 peak in naphthylamine is due to the sequential loss of hydrogen followed by a mass 27 loss. It will be shown below with computational findings that the most likely channel behind the peak at m/z 115 is the loss of a single HCNH unit in both the molecules. Apart from these peaks, there exists a minor peak [depicted in the inset of Fig. 3(a)] at m/z 128 (loss of mass 15 amu neutral) in the case of methyl-quinoline and m/z 126 (loss of mass 17 amu neutral) in the case of naphthylamine. At higher photon energies [depicted in the inset of Fig. 3(b)], an additional peak at m/z 127 (loss of mass 16 amu neutral) also appears in the mass spectra of naphthylamine. Considering the nature of the functional groups attached to the two targets, the peak at m/z 128 in methyl-quinoline is assigned to the loss of CH₃ neutral from the parent, while the peaks at m/z 126 and 127 in naphthylamine are assigned to the loss of NH₃ and NH₂ neutrals from the parent, respectively.

The branching ratios for the mass 143 isomers are depicted in Fig. 3(c). The contributions from the peaks at m/z 115 and 116 could not be resolved and hence are represented together with the hypothesis that contributions from the 116 channel would be minor. Figure 3(c) also contains the branching ratio of the hydrogen loss channel (in the case of methyl-quinoline) and the substituent losses (126 in the case of naphthylamine and 128 in the case of methyl-quinoline). Of all the channels considered in both the molecules, the hydrogen loss in methyl-quinoline⁺ is the first to open at ~ 12.5 eV. At around 13 eV, the 115 curve in methyl-quinoline has its onset, while the same curve in naphthylamine has its onset at a slightly higher energy. The 115 curve in both molecules is the most intense channel. The curve corresponding to naphthylamine rises more rapidly leading to a small difference between the two curves in the energy range of 15–17.5 eV, beyond which both curves tend to coincide. This suggests the presence of a minor channel at lower energy exclusive to naphthylamine, which then is rapidly overtaken by a channel that is common to both molecules. The neutral fragment lost in this case is either 27 or 28; both of these masses most likely contain nitrogen, which in naphthylamine is part of substituent, while in methyl-quinoline is part of the main ring. Considering that both molecules appear to lose this neutral fragment in a similar

fashion along with the fact that both molecules have very different structures, especially when it comes to the nature of nitrogen is an indication of both molecules isomerizing to common isomers prior to dissociation. Finally, the channels leading to m/z 128 and 126 open at an energy slightly larger than the one of m/z 115 and remains a minor channel in the entire energy range in both molecules.

In order to better understand the nature of the m/z 115 peak, an attempt is made by sampling the ions detected in coincidence with electrons detected at various radii (rings) in the VMI detector, which in essence is sampling ions decaying at different binding energies. In this context, the evolution of the mass spectra in the region covering $m/z = 115$ and 116 was analyzed with increasing radii of electron detection. A representative example of the evolution of the ion peaks in both molecules normalized to their peak value is depicted in Figs. 4(a)–4(c). As can be seen in all three figures, in the case of methyl-quinoline, the peak remains close to $m/z = 115$ with minor shifts with increasing radii (decreasing internal energy). The same observation is seen in the case of naphthylamine [Figs. 4(a) and 4(b)] except in the case of the final ring [Fig. 4(c)], with an abrupt shift in the peak close to $m/z = 116$. Indeed, excluding this final ring, the profile of the peaks is similar in both molecules. This again confirms that in the energy range sampled, the dynamics of the 115 channel is very similar in both molecules, except in a very small energy regime with the least binding energy.

C. Reaction pathways

Pathways that may explain the origin of the peaks in the mass spectra is discussed in this section. During the study, it was found that certain channels are exclusively accessible only after initial isomerizations. Such observations that are purely computational are gradually brought forth to bring out a comprehensive overview of the potential energy surface compatible with the experimental trends. The case of quinoline and isoquinoline is described first, followed by the case of naphthylamine and methyl-quinoline.

1. Mass 129 isomers

The potential energy surface of quinoline has been extensively explored in previous studies,^{33,51} hence, more focus is given to the dissociative pathways of isoquinoline. A few pathways producing HCN from isoquinoline has been reported earlier.¹⁸ However, it has been demonstrated in quinoline³³ that seven member isomerization pathways not considered in other studies play a very important role for the fate of the dissociating molecule. Hence, similar isomerization pathways are explored for isoquinoline. Four such pathways were found for isoquinoline leading to Cyclopenta[c]azepine (c-CPA), Cyclopenta[d]azepine (d-CPA), cyclohexa[b]pyrrole (b-CHP), and cyclohexa[c]pyrrole (c-CHP). Two of these isomers (c-CPA and b-CHP) are the same two isomers that quinoline isomerizes and are the isomers in which it was shown theoretically that HCN and C_2H_2 loss occurs preferentially. New pathways for the HCN and HNC loss from d-CPA and C_2H_2 loss from c-CHP were explored for the first time (the latter driven by the observation that C_2H_2 is lost preferentially from the non-nitrogen containing ring in quinoline). For the case of HCN loss, all pathways explored including the ones reported earlier are very close in energy (the highest transition states in the different HCN pathways are within ~ 0.25 eV of each other) and cannot be discriminated on pure energetics. The same observation holds for the cases of HNC loss and C_2H_2 loss

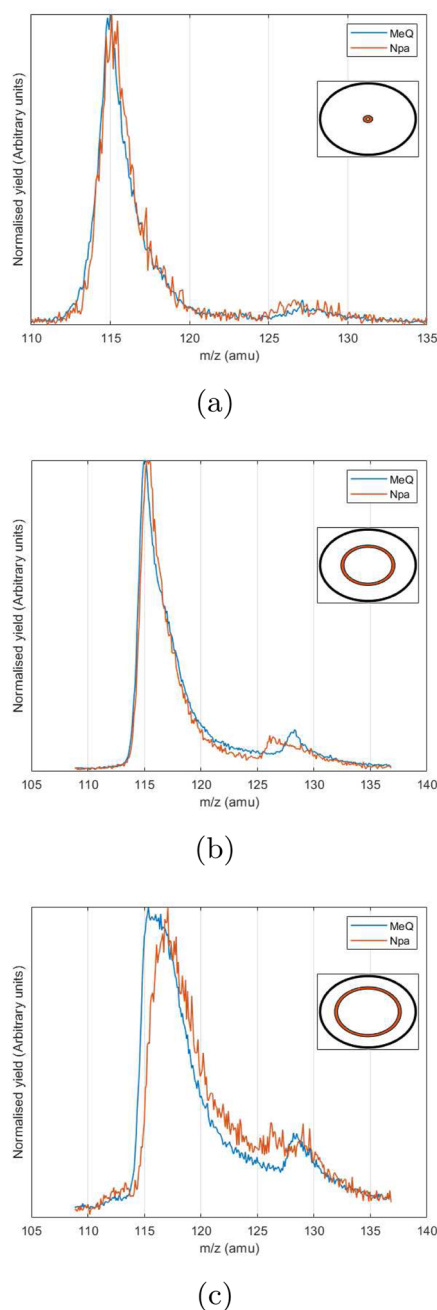


FIG. 4. Ions detected in coincidence with electrons sampled from rings of varying radii from the positional information of the electrons on the VMI detector. (Insets figuratively represented the rings from which the electrons were sampled.)

too. So, while the three sets of pathways do vary significantly in energy (the highest transition states in C_2H_2 pathways is ~ 1 eV and the highest transition states in the HNC pathways is ~ 0.5 eV more than the highest transition states in the HCN pathways), which explains the different energy onsets seen in the experiment, within

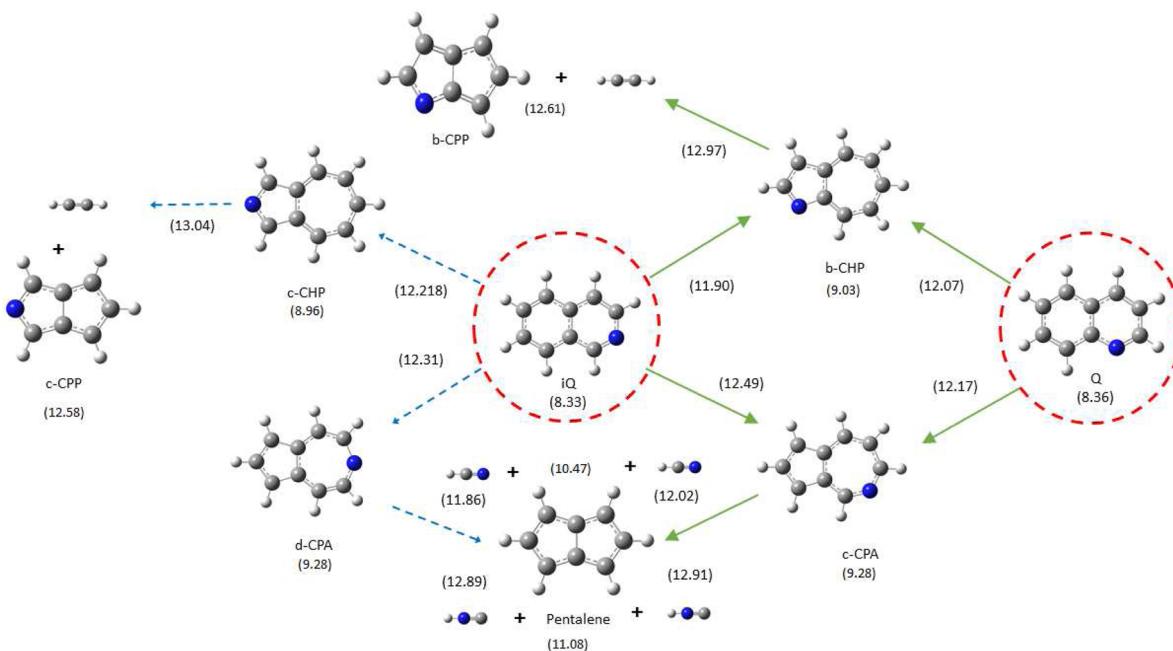


FIG. 5. Summary of isomerization and further dissociation pathways for mass 129 isomers (energies are in eV and are relative to neutral quinoline).

each set, they are quite comparable in energy. Hence, the pathways within each set cannot be discriminated on their energetics alone. While a full RRKM modeling of the pathways is beyond the scope of the present work, the similarities seen in the mass spectra and, more importantly, the branching ratios of the two molecules can be evoked to reasonably predict the role of each of these pathways in the experiment. The above-mentioned similarities can be explained if the kinetics of the pathways underneath would be the same for both molecules. This then would imply that the decay channels proceed via the same isomer in both molecules, which in this case is c-CPA for HCN loss and b-CHP for C_2H_2 loss. Likewise, the HNC channel would only contribute negligibly to the 102 peak in isoquinoline, as it was found to occur in the case of quinoline.³³

The summary of the isomerization and further dissociation pathways is shown in Fig. 5, with the highest barrier in each step given along with the arrows connecting the different structures. The most probable pathway based on experimental evidence is indicated by the solid arrows. Note that isoquinoline has other dissociating pathways from c-CHP and d-CPA; however, those pathways can be safely assumed to not contribute majorly because those pathways did not play a major role in the photodissociation of quinoline.³³ In this way, experimental observations can be used to discriminate among various theoretical predictions.

2. Mass 143 isomers

Detailed potential energy surface explorations are carried out for the channels seen in the experimental spectra for Npa and MeQ. The losses of neutral fragment considered are the hydrogen loss, substituent losses (CH_3 , NH_3 , NH_2), hydrogen cyanide loss, hydrogen

isocyanide loss, and the methyl amidogen loss. These are channels that are assumed to participate in the decay of these isomers. The complete reaction pathways are reported in the supplementary material, and brief summaries are as follows.

a. Hydrogen loss. The hydrogen loss channels in Npa+ and MeQ+ are computationally investigated and the results are as follows: Table I reports the product energies of the various mass 142 isomers with respect to naphthylamine neutral. No transition state was found in the final dissociating step at the level of theory considered here, so the energy of the products is reported as the barrier for the hydrogen loss energy, except in the case of combination C4 wherein the isomerization barrier was higher (isomerization barrier reported in parenthesis). The difference in the energies of the different combinations taken here is quite significant. Each of these combinations represents hydrogen loss from some of the key intermediates in other neutral loss pathways. The most energetically expensive positions from which the hydrogens can be lost are from the carbons in the main ring (be it six membered or seven membered) as they cause deformations in the accompanying ion. This could be because of the change in hybridization of carbon to sp , which causes significant bond strain on the system as the sp carbon prefers to be linear. On the other hand, if the hydrogen is lost from the methyl group in MeQ+, the cost in energy is quite low, which is in line with previous observations. The nitrogen in the ammine group in Npa+ however is an sp^2 site as evidenced by its planar nature; hence, the loss of hydrogen from it is more energetically demanding than hydrogen loss from the methyl group in MeQ+. The next set of energetically low combinations correspond

TABLE I. Product energies (with respect to naphthylamine neutral) for different combinations of 142 isomers. Numbers in parenthesis in first column denote position from which the hydrogen was lost (see Figs. 1 and 6 for position labels). Number in parenthesis in second column denote the energy of the transition state in the pathway to the product if it is higher than the final dissociating step.

Combination	Products	Energy (eV)
C1	[MeQ - H(4)] + H	12.61
C2	[CH ₂ -quinoline] + H	10.90
C3	[1BN - H(3)] + H	12.44
C4	[1BN - H(1)] + H	10.91(11.74)
C5	[2BN - H(2)] + H	10.82
C6	[2BN - H(1)] + H	12.54
C7	[2-cyano-1-indene] + H	10.67
C8	[2Npa - H(3)] + H	12.52
C9	[NH ₂ -naphthalene] + H	11.19

to hydrogen loss from stable intermediates in the other dissociation mechanisms. C7 represents hydrogen loss from the penultimate intermediate (2H-2-cyano indene) in the HNC pathway. However, the cost of losing the HNC is less than the one to lose hydrogen by 0.76 eV. Hence, it is suggested that if the molecule deforms to the final intermediate, the molecule would rather lose HNC than H. C5 represents hydrogen loss from the nitrogen in 2BN+. While the cost of losing hydrogen is cheaper than the cost of losing HCNH from 2BN, the lack of hydrogen loss peak in the experimental spectra of Npa suggests this is not an important pathway either. These arguments agree quite well with the experimental observations. Methyl-quinoline shows substantial hydrogen loss due to the sp³ carbon in its methyl substituent.

b. Substituent losses. The loss of ammonia from Npa, which is responsible for its peak at $m/z = 126$, follows a fairly straightforward pathway, starting with a direct hydrogen migration from one of the neighboring carbons followed by a cleavage of the formed NH₃ substituent, which again occurs in a barrier less fashion as it involves a simple bond cleavage. The products so formed are higher than the reaction barriers of the other major channels (H, HCNH, HNC, HCN). This corroborates very well with the experiment where it is seen that the NH₃ channel is a minor channel. Furthermore, the appearance of a direct NH₂ loss channel at higher photon energy spectra and with a lower intensity than the NH₃ indicates that the molecule prefers to lose NH₃. This strongly indicates the role of hydrogen migration in further dissociation. This agrees very well with the computational findings, wherein the barrier to direct NH₂ loss is around 0.6 eV higher than the barriers to NH₃ loss (see the supplementary material). The role of hybridization of the dissociating fragment is also seen from the case of Npa, where hydrogen migration allowed the nitrogen to change its hybridization from sp² to sp³, while the carbon in methyl group of methyl-quinoline was already sp³ in the first place. Thus, the loss of the intact CH₃ unit was seen in the mass spectra of methyl-quinoline where its sp³ carbon allowed it to dissociate without any structural rearrangements. At the same time, both these channels are very minor channels, indicating that structural deformations are necessary for profuse fragmentation.

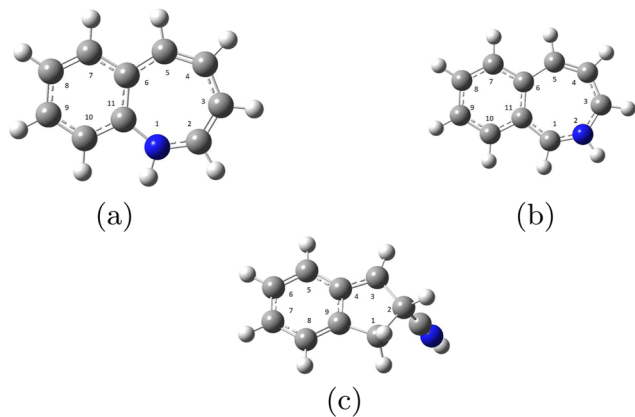


FIG. 6. (a) 1H-1-Benzazepine (1BN+), (b) 2H-2-Benzazepine (2BN+), and (c) 2H-2-Cyano Indene (2HCI+).

c. Isomerizations. Past studies have indicated that often a parent molecular ion undergoes isomerization before dissociation,^{32,33,35} and hence isomerization reactions have to be considered to fully describe the dissociative landscape. Apart from isomers that vary in the relative position of the substituent group, benzazepines are another class of molecules that both MeQ and Npa can isomerize. The structures of the benzazepines 2H-2-Benzazepine (2BN+) and 1H-1-Benzazepine (1BN+), which are considered in our study, are shown in Fig. 6.

The substituent (the amine group in the case of Npa+ and the methyl group in the case of MeQ+) attached to the parent ring is first pushed inward followed by a ring expansion to the seven membered azepine ring. A number of hydrogen migrations facilitates this process. For instance, in the case of MeQ+, the CH₃ group is sterically hindering to begin with; hence, a hydrogen migration is done first to the attached carbon before the CH₂ group is incorporated into the ring. In the case of MeQ+, there are two possibilities in the rotation of the CH₂ group, leading to different hydrogen shifted 1-benzazepines. Once the CH₂ group is incorporated into the parent ring, further hydrogen migrations are made until the nitrogen is hydrogenated; thus, both possibilities would ultimately give rise to the same 1BN+. In the case of Npa+, however, the two rotations would give rise (after the migrations and the expansion) to different isomers, 2BN+ and 3BN+. Of these two isomers, only pathways to 2BN+ successfully converged. The two pathways that converged differ in the order of hydrogen migration. The higher energy pathway with its highest transition state 12.64 eV consists of incorporating the NH₂ group followed by a hydrogen migration to form 2BN+. The lower energy pathway starts with hydrogen migrations followed by the inclusion of the NH group with its highest transition at a significantly lower 10.36 eV. Another pathway connecting 1BN+ and 2BN+, which proceeds via Cyclohepta[1,2-b]pyridine (b-CPY), was also found with energetics quite similar to the original isomerization. This pathway therefore brings both molecules to common ground via isomerization to 1BN+ and 2BN+. Furthermore, another isomerization scheme to a five membered ring containing isomer, 2H-2-Cyano Indene (2HCI+) was also found exclusive to Npa+. This isomer was found key to HNC loss as explained below.

Having found different isomers of the two molecules, HCN, HNC, and HCNH losses from these isomers and the parents are explored.

d. HCN loss. In the case of HCN loss from the mass 143 isomers, based on the insights from the quinoline studies, the possible accompanying larger fragments can be indenenes or propynylbenzene. The latter is energetically more expensive than the former (around 1.1 eV). Furthermore, the pathways to produce the latter directly from unisomerized Npa⁺ and MeQ did not converge successfully. Thus, the HCN loss from the benzazepines were investigated. The first step would be hydrogen migrations, wherein the hydrogen from the nitrogen would have to migrate to another site. Here, it was seen that immediate migration to adjacent sites would not allow the ring to contract, which is expected due to the sp³ nature of the carbon (with the migrated hydrogen), which cannot form one more bond (and hence a HCN loss from 3BN⁺ is not expected). The only contraction that did converge involved the tertiary carbon with the hydrogen migrating to alpha carbon next to other tertiary carbon. This is also quite reasonable because this is the site that offers the least steric hindrance to ring closure.

e. HNC loss. In the case of MeQ⁺ and Npa⁺, attempts to lose HNC from the benzazepine structures failed mostly after the ring contractions with the next expected transition states failing to converge. However, a pathway similar to the loss of HNC from aniline⁵² was attempted here for Npa, and this has converged. This route involves isomerization to a five member ring containing 2H-2-cyano indene first prior to HNC abstraction. Here, note that in the final step, the transition state while lower in energy than the products is very close to its energy (only a difference of 0.02 eV). This discrepancy with the transition state being lower than the products could be rectified if a more computationally expensive calculation was carried out; however, the difference between the energies is not expected to change drastically. These energetics also point toward the potential energy surface being almost flat at the dissociating step. Note that this pathway is energetically significantly lower (around 1 eV) than the pathways losing HCN discussed previously. Similar attempts to lose HNC from MeQ⁺, however, were not successful with structures after the breakage of the main ring failing to converge.

This again sits well with experimental results in the context of a lower energy channel that exists in Npa, which does not contribute as much in MeQ. This channel could very well be the HNC loss channel that Npa shows, which MeQ seemingly does not show.

Also note that in case of both molecules and for either of the mass 27 neutral losses, the accompanying ion is the same indene cation.

f. HCNH loss. In the case of Npa⁺, initially the loss of H₂NC and HCNH (which involved a hydrogen migration first) directly from Npa⁺ was attempted. Both these pathways ended in transition states from which H₂NC (or HCNH) could not be lost. Loss of H₂NC requires least structural rearrangement at first glance since both hydrogens are attached to N. However, a ring contracted intermediate involving a five-membered ring attached to H₂NC could not be obtained. A HCNH loss pathway from 2HCl⁺, which involves two further hydrogen migrations after the formation of 2HCl⁺, converged. Similarly pathways leading to the loss of a mass 28 neutral from MeQ did not converge either.

Attempts to look for the loss of HCNH following isomerization to 1BN⁺ and 2BN⁺ were also successful. In the pathway starting from 2BN⁺, note that the transition state in the final step is energetically lower than the final product. However, while there are other cases in which the transition state has been lower in energy than the following intermediate, their difference has never been more than 0.01 eV, while in this case it is significantly higher. This is most likely an artifact due to improper accounting of electrons on the departing fragments as evidenced by checking the Mulliken charge or the APT charge on the departing fragment. This can be resolved if constrained density functional theory (DFT) calculations⁵³ are carried out. Note that such calculations would change the energetics and not the mechanism⁴⁰ and hence have not been carried out currently. The pathway from 1BN⁺ proceeds in an identical manner to the pathway from 2BN⁺; however, the final dissociating transition state is higher in energy. In both cases, the loss of HCNH leads to the formation of the indenyl cation.

Having found all the necessary pathways, we took a closer look at them. In the case of Npa, the HNC pathway is the least in barrier heights. HCNH from Npa⁺ can be lost either from the five membered 2HCl⁺ or from the seven membered 2BN⁺. The barrier of both these processes are the product energies itself. The isomerization processes themselves are also comparable in energy (with isomerization to 2BN⁺ being 0.15 lesser than isomerization to 2HCl⁺). If the molecule isomerizes to 2HCl⁺, the energetic cost of losing HNC is 1.55 eV lower than the cost of losing HCNH, and hence it would rather lose HNC instead. So, if Npa⁺ does majorly isomerize to 2HCl⁺, it would profusely lose HNC and thus would have reflected as a major peak at m/z 116 in the experimental spectra, which is not the case. Thus, a major portion of Npa is suggested to isomerize to 2BN⁺ prior to HCNH abstraction, while the remaining minor fraction that isomerize to 2HCl⁺ loses HNC instead. In the case of methyl-quinoline, no lower energy pathway was found, which corroborates well with the experimental exclusivity of the lower channel for Npa. The HCNH pathway from 1BN⁺ and the corresponding HCN pathway from the same are comparable (unlike in the case of Npa, where the HCNH pathway from 2BN⁺ is energetically cheaper than the corresponding HCN pathway by at least 0.4 eV). However, the isomerization pathway connecting 1BN⁺ and 2BN⁺ is also comparable with these two dissociating channels. This combined with the fact 2BN⁺ easily loses HCNH, and the fact the experimental observations hint toward the 115 peak originating from the same isomer suggests that MeQ too loses HCNH from 2BN⁺. However, the possibility that 2-BN⁺ can also isomerize to 1-BN⁺ and then dissociate, although unlikely considering it easily loses HCNH, cannot be ruled out conclusively. Nevertheless, the loss of HCNH is suggested to proceed via one of the two benzazepines, which both molecules can isomerize, agrees well with our experimental inferences.

For the fate of the 115 peak, we also computationally explore the energetics of different 115 + 27 + 1 combinations (sequential loss of mass 27 isomer followed by hydrogen loss). The other combination of 115 + 1 + 27 (sequential loss of hydrogen followed by mass 27 neutral) was ruled out as the energetics of the structures involved in the process is well above the other pathways considered. For the case of Npa, if the hydrogen was lost after HNC, it would require around 12.8 eV. If the hydrogen was lost after HCN was lost, it would require around 12.2 eV. However, from the same isomer,

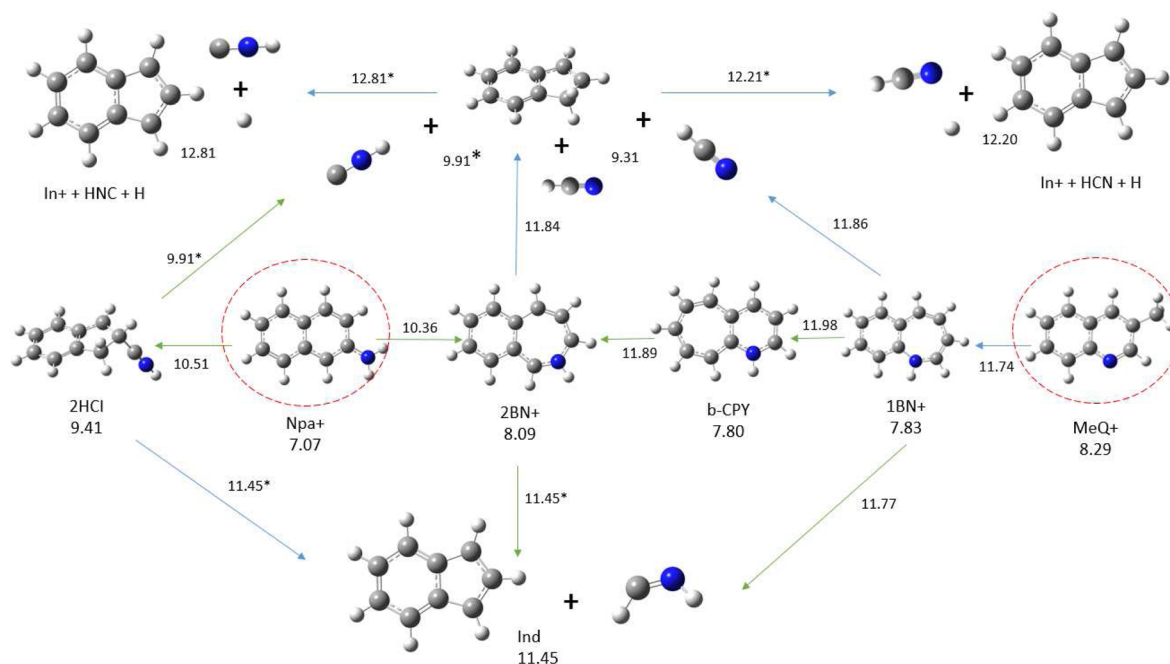


FIG. 7. Summary of the isomerization and further dissociation pathways for mass 143 isomers. Energies in eV and are relative to neutral Npa. (Energies marked with * are the energies of the products as the energy of the highest transition state in those pathways were found to be lower than the products; see the text for more details.)

the loss of HCNH requires lesser energy 0.76 eV lesser. For the case of MeQ, the energetics are similar to that of Npa for the loss of HCN followed by hydrogen loss. Considering that the mass 115 peak in both molecules must have arose via similar dynamics, the combination of HNC and hydrogen is unlikely as that channel is closed for MeQ. Of the remaining two combinations, the loss of HCNH from 2-BN+ is the most likely to occur energetically. Furthermore, the energetics computed here assume that the mass 27 neutral fragment carries no internal energy, i.e., it is lost in a vibrationally cold manner, which is highly unlikely. Hence, the actual practical barriers to sequential losses would be higher than the ones computed. Altogether, it is strongly suggested that the mass 115 peak in both molecules is due to the loss of HCNH via 2BN+ (or 1BN+) they isomerize. This may why the 115 channel opens at a higher energy, but once the dissociation barrier is crossed, it loses HCNH with high efficiency, leading to the overwhelming dominance of the 115 peak.

The summary of the isomerization and further dissociation pathways along with sequential losses for the 115 peak is shown in Fig. 7, with the highest barrier in each step given along with the arrows connecting the different states. The most probable pathways based on experimental evidence are indicated by the solid arrows.

V. DISCUSSION

Evidence of isomerization prior to dissociation has been unearthed in the past. In a vast majority of those cases, these isomerizations were involved seven member isomerization mechanisms that controlled the fate of the dissociating molecule. Azulene,

the isomer that naphthalene was concluded to isomerize (Refs. 31 and 32) prior to acetylene abstraction, is a seven member ring containing the isomer. This was recently reaffirmed independently by another group wherein it was concluded via analysis of kinetic energy release distributions measurements⁵⁴ that the ions accompanying acetylene abstraction was majorly pentalene with another minor product being phenylacetylene. Incidentally, these are the same products that are suggested to form after HCN abstraction from quinoline too.³³ Tropylium, which was experimentally identified to be the product formed after hydrogen abstraction from toluene,⁵⁵ is yet again a seven membered ring. Furthermore, tropylium derived structures were identified to be the hydrogen loss products from methyl naphthalene too.⁵⁶ The nitrogenated analog to the tropylium derived structures would be benzazepine derived structures that arise in PANH dissociation. For instance, quinoline³³ is strongly suggested to prefer the isomerization route to seven member structures c-CPA and b-CHP, prior to dissociation in the case of both HCN and C₂H₂ losses. In a study into the photodissociation of acridine and phenanthridine, the product ions accompanying HCN loss were experimentally identified to be acenaphthylene and benzopentalene, and products that were shown to be formed only after the parent molecules undergo ring expansion to a common benzazepine derived isomer.³⁵ A similar evidence was unearthed independently by another group with an experiment probing the photodissociation of anthracene and phenanthrene, where the product accompanying C₂H₂ loss in both molecules was experimentally identified to be yet again acenaphthylene, along with possible minor contributions from benzopentalene.⁵⁷ These evidence put together

point to startling similarity behind the dissociative dynamics of both PAHs and PANHs as seen from the case of quinoline and naphthalene, and the case of acridine, phenanthridine and anthracene, phenanthrene. This similarity could be in fact be seven member isomerizations that seem to underline the common processes found. On a related note, in the case of graphene, theoretical and experimental evidence⁵⁸⁻⁶⁰ have been recently uncovered, wherein its edge states were shown to be preferably in a “reczag” configuration, consisting of fused pentagonal and heptagonal rings over the conventional armchair or zigzag configurations with hexagonal rings.

The current experimental results along with the computational findings also point toward these seven member isomerizations playing an important role in the photodissociation of quinoline, isoquinoline, methyl-quinoline, and Npa too. In the case of quinoline and isoquinoline, the isomerization proceeded via a ring expansion mechanism, pathways structurally similar to the naphthalene–azulene isomerization. However, in the case of Npa and MeQ, the substituent (both the ammine group and the methyl group) gets incorporated into the main parent ring to form the seven member structure. This ubiquity of these seven member ring isomers in all these aforementioned molecules, irrespective of their different structures and the different mechanisms to form them, hints toward a more fundamental role these isomers play in the dissociative chemistry of these molecules and is strongly suggestive of a universality in their fragmentation trends of PA(N)Hs in general. Indeed, while evidence pointing toward isomerizations have existed before, they were scattered, and to the best of the authors’ knowledge, the present study is the first to provide a comparative study across different targets, combining facets of theory and experiment to bring forth the seven member isomerization mechanism to the center stage.

While the seven membered ring containing isomers seems to play an important role in dissociation, there exists counter-examples too. For instance, a theoretical study concluded that while the seven member mechanism prior to dissociation was important in cata-condensed systems, such as naphthalene, azulene, anthracene, phenanthrene, and tetracene, it was found to be energetically expensive in the case of a bigger peri-condensed system, such as pyrene.⁶¹ Similarly, in another study with methyl substituted pyrene, it was again found that the seven membered isomerization scheme was not concluded to contribute majorly in the molecule’s photodissociation.⁶² Effects like ring strain in higher ring peri-condensed systems, which seem to prohibit the formation of seven member ring containing intermediates, have to be investigated in more detail.

Another important mechanistic aspect that seems to play a crucial role in dissociation, is hydrogen migration. In the past, hydrogen migrations have been known to precede sequential and molecular hydrogen losses.³⁶⁻³⁸ In the current study, we see that hydrogen migration plays a role in the loss of larger neutrals too. In the case of the mass 129 isomers, the ring expansion to the seven member isomerizations starts with hydrogen migrations to the tertiary carbon. For further dissociation in the case of quinoline, HNC loss would have been facilitated by a hydrogen migration to the nitrogen; however, this channel was shown to contribute only in negligible proportions.³³ With the similarities between the experimental signatures of isoquinoline and quinoline unearthed in this study, we can safely assume that contribution of a HNC loss channel would be

negligible for isoquinoline too. Furthermore, a HCNH channel, which would have been possible provided multiple hydrogen migrations had occurred, is also not seen at all in both molecules. In the case of the mass 143 isomers, hydrogen migrations facilitate the formation of the benzazepines isomers. Once the isomer is formed, further hydrogen migrations would have led to HCN loss; however, it is seen that the molecules instead loses HCNH profusely. It seems that a delicate balance between the movement of hydrogen across the ring and the breakage of the ring exists and this controls the fate of the dissociating molecule. This aspect requires further investigation.

The products formed as a result of the mechanisms discussed here are of great astrophysical significance. Indene, identified to be a minor product formed after mass 27 neutral loss from the mass 143 isomers from the current experiment, was directly detected in TMC-1 very recently.⁶³ Indenyl, which is assigned to the dominant 115 peak in MeQ and Npa, in its neutral form is a resonance stabilized radical, which is known to be important precursors in PAH growth⁶⁴ in conditions relevant to interstellar chemistry. More specifically, reactions of indenyl with other smaller hydrocarbons have led to the formation of naphthalene,⁶⁵ phenanthrene, anthracene, benzo-fulvalene,⁶⁶ and other bigger organics.⁶⁷ Dissociative recombination with electrons of HCNH⁺ (which in its neutral form is produced profusely in the current experiment from the photodissociation of Npa and MeQ) is proposed to be one of the important sources for both HCN and HNC in the interstellar medium.^{68,69} It is clear that the photodissociation of PANHs leads to a rich variety of important organics. The current results, which suggests the seven member isomerization as a crucial mechanism controlling these photodissociation products, would greatly benefit future studies on this topic.

VI. CONCLUSION

In summary, the PEPICO spectrum of two pairs of PANH isomers, quinoline–isoquinoline and 2-naphthylamine-3-methyl-quinoline, have been measured using the velocity map imaging technique. Complementary structure calculations were also carried out, which were instrumental in assigning the channels observed in the experimental spectra. The primary dissociation channels of the m/z 129 isomers are found to be hydrogen loss, hydrogen cyanide loss, acetylene loss, and cyanoacetylene loss. For the mass 143 isomers, methyl amidogen loss was identified to be the dominant primary channel in both molecules. A lower energy hydrogen isocyanide channel was found to be exclusive to naphthylamine, while methyl-quinoline possess an exclusive lower energy hydrogen loss channel. Apart from these channels, there also exists a minor hydrogen cyanide channel, which is again common to both molecules. Comparison of experimental signatures of the four molecules reveals several similarities highly indicative of common dissociative mechanisms underneath and revealed insights into the way the aforementioned neutrals could have been lost. In all four cases, isomerization is suggested to occur prior to dissociation of the major channels, with the m/z 129 isomers isomerizing to either cyclopenta[c]azepine or cyclohexa[b]pyrrole before hydrogen cyanide or acetylene abstraction and the m/z 143 isomers isomerizing to 2H-2-benzazepine and 1H-1-benzazepine prior to methyl amidogen or hydrogen cyanide abstraction. In addition to these aforementioned channels, another five membered isomerization

channel was found in the case of Npa⁺, which also seems to play a role in its dissociation, especially in the case of HNC loss, although the seven membered isomerization seems to be omnipresent in the present study. The fundamental role the isomerization mechanisms plays in photodissociation of PANHs was brought forth both experimentally and computationally. The generalization of the isomerization mechanism to systems with higher rings is an aspect that requires further investigation. Furthermore, the quantum chemical implications of these seven member ring containing intermediates would also have to be explored further to completely unravel the mechanistic attributes that control the statistical dissociation of these molecules.

SUPPLEMENTARY MATERIAL

The supplementary material contains detailed descriptions of all the pathways reported in this manuscript. It also contains the photoelectron spectra of the four target molecules, positional information of ions, and mass selected binding energy curves of important channels.

ACKNOWLEDGMENTS

The authors acknowledge the support provided by the 2022-024 Indo-Italian Program for Exchange of Researchers “Genesis of organic molecules in the extra-terrestrial environment: role of energetic radiation” and the funds provided by a grant from the Italian Ministry of Foreign Affairs and International Cooperation and the Indian Department of Science Technology.

AUTHOR DECLARATIONS

Conflict of Interest

The authors have no conflicts to disclose.

Author Contributions

Arun S: Conceptualization (equal); Data curation (equal); Formal analysis (equal); Investigation (equal); Visualization (equal); Writing – original draft (equal). **Karthick Ramanathan:** Conceptualization (equal); Investigation (equal); Methodology (equal); Writing – review & editing (equal). **Muthuamirthambal Selvaraj:** Conceptualization (equal); Formal analysis (equal); Investigation (equal); Writing – review & editing (equal). **Marco Causero:** Methodology (equal); Software (equal). **Robert Richter:** Data curation (equal); Formal analysis (equal); Investigation (equal); Methodology (equal); Resources (equal). **Nitish Pal:** Investigation (equal); Resources (equal). **Jacopo Chiarinelli:** Data curation (equal); Formal analysis (equal); Investigation (equal); Methodology (equal); Software (equal). **Paola Bolognesi:** Conceptualization (equal); Formal analysis (equal); Investigation (equal); Methodology (equal); Project administration (equal); Writing – review & editing (equal). **Lorenzo Avaldi:** Conceptualization (equal); Funding acquisition (equal); Investigation (equal); Project administration (equal);

Writing – review & editing (equal). **M. V. Vinitha:** Conceptualization (equal); Investigation (equal); Methodology (equal); Writing – review & editing (equal). **Chinmai Sai Jureddy:** Investigation (equal). **Umesh R. Kadhane:** Conceptualization (equal); Funding acquisition (equal); Investigation (equal); Project administration (equal); Resources (equal); Supervision (equal); Writing – review & editing (equal).

DATA AVAILABILITY

The data that support the findings of this study are available from the corresponding author upon reasonable request.

REFERENCES

- ¹H. I. Abdel-Shafy and M. S. Mansour, “A review on polycyclic aromatic hydrocarbons: Source, environmental impact, effect on human health and remediation,” *Egypt. J. Pet.* **25**, 107–123 (2016).
- ²H. Richter and J. Howard, “Formation of polycyclic aromatic hydrocarbons and their growth to soot—A review of chemical reaction pathways,” *Prog. Energy Combust. Sci.* **26**, 565–608 (2000).
- ³M. Frenklach and A. M. Mebel, “On the mechanism of soot nucleation,” *Phys. Chem. Chem. Phys.* **22**, 5314–5331 (2020).
- ⁴A. Tielens, “Interstellar polycyclic aromatic hydrocarbon molecules,” *Annu. Rev. Astron. Astrophys.* **46**, 289–337 (2008).
- ⁵A. G. G. M. Tielens, “The molecular universe,” *Rev. Mod. Phys.* **85**, 1021–1081 (2013).
- ⁶F. Salama, G. A. Galazutdinov, J. Krelowski, L. Biennier, Y. Beletsky, and I.-O. Song, “Polycyclic aromatic hydrocarbons and the diffuse interstellar bands: A survey,” *Astrophys. J.* **728**, 154 (2011).
- ⁷A. Li, “Spitzer’s perspective of polycyclic aromatic hydrocarbons in galaxies,” *Nat. Astron.* **4**, 339–351 (2020).
- ⁸V. Vuitton, R. Yelle, and M. McEwan, “Ion chemistry and N-containing molecules in Titan’s upper atmosphere,” *Icarus* **191**, 722–742 (2007).
- ⁹D. P. Cruikshank, E. Wegryn, C. Dalle Ore, R. Brown, J.-P. Bibring, B. Buratti, R. Clark, T. McCord, P. Nicholson, Y. Pendleton, T. Owen, G. Filacchione, A. Coradini, P. Cerroni, F. Capaccioni, R. Jaumann, R. Nelson, K. Baines, C. Sotin, G. Bellucci, M. Combes, Y. Langevin, B. Sicaudy, D. Matson, V. Formisano, P. Drossart, and V. Mennella, “Hydrocarbons on Saturn’s satellites Iapetus and Phoebe,” *Icarus* **193**, 334–343 (2008), Saturn’s Icy Satellites from Cassini.
- ¹⁰B. A. McGuire, R. A. Loomis, A. M. Burkhardt, K. L. Lee, C. N. Shingledecker, S. B. Charnley, I. R. Cooke, M. A. Cordiner, E. Herbst, S. Kalenskii, M. A. Siebert, E. R. Willis, C. Xue, A. J. Remijan, and M. C. McCarthy, “Detection of two interstellar polycyclic aromatic hydrocarbons via spectral matched filtering,” *Science* **371**, 1265–1269 (2021).
- ¹¹E. Peeters, H. W. W. Spoon, and A. G. G. M. Tielens, “Polycyclic aromatic hydrocarbons as a tracer of star formation?,” *Astrophys. J.* **613**, 986–1003 (2004); [arXiv:astro-ph/0406183](https://arxiv.org/abs/astro-ph/0406183) [astro-ph].
- ¹²O. Berné and A. G. G. M. Tielens, “Formation of buckminsterfullerene (C₆₀) in interstellar space,” *Proc. Natl. Acad. Sci. U. S. A.* **109**, 401–406 (2011).
- ¹³J. Zhen, P. Castellanos, D. M. Paardekooper, H. Linnartz, and A. G. Tielens, “Laboratory formation of fullerenes from PAHs: Top-down interstellar chemistry,” *Astrophys. J.* **797**, L30 (2014).
- ¹⁴M. S. Murga, V. V. Akimkin, and D. S. Wiebe, “Efficiency of the top-down polycyclic aromatic hydrocarbon-to-fullerene conversion in ultraviolet irradiated environments,” *Mon. Not. R. Astron. Soc.* **517**, 3732–3748 (2022), <https://academic.oup.com/mnras/article-pdf/517/3/3732/46651131/stac2926.pdf>.
- ¹⁵M. S. Gudipati and R. Yang, “In-situ probing of radiation-induced processing of organics in astrophysical ice analogs—Novel laser desorption laser ionization time-of-flight mass spectroscopic studies,” *Astrophys. J.* **756**, L24 (2012).
- ¹⁶J. Pety, D. Teyssier, D. Fossé, M. Gerin, E. Roueff, A. Abergel, E. Habart, and J. Cernicharo, “Are PAHs precursors of small hydrocarbons in photo-dissociation regions? The Horsehead case,” *Astron. Astrophys.* **435**, 885–899 (2005).

- ¹⁷V. V. Guzmán, J. Pety, J. R. Goicoechea, M. Gerin, E. Roueff, P. Gratier, and K. I. Öberg, "Spatially resolved $I-C_3H^+$ emission in the Horsehead photodissociation region: Further evidence for a top-down hydrocarbon chemistry," *Astrophys. J.* **800**, L33 (2015).
- ¹⁸J. Bouwman, B. Sztáray, J. Oomens, P. Hemberger, and A. Bodi, "Dissociative photoionization of quinoline and isoquinoline," *J. Phys. Chem. A* **119**, 1127–1136 (2015).
- ¹⁹U. R. Kadhane, M. V. Vinitha, K. Ramanathan, A. S. J. Bouwman, L. Avaldi, P. Bolognesi, and R. Richter, "Comprehensive survey of dissociative photoionization of quinoline by PEPICO experiments," *J. Chem. Phys.* **156**, 244304 (2022).
- ²⁰J. ORÓ, "Mechanism of synthesis of adenine from hydrogen cyanide under possible primitive earth conditions," *Nature* **191**, 1193–1194 (1961).
- ²¹D. Roy, K. Najafian, and P. von Ragué Schleyer, "Chemical evolution: The mechanism of the formation of adenine under prebiotic conditions," *Proc. Natl. Acad. Sci. U. S. A.* **104**, 17272–17277 (2007).
- ²²V. P. Gupta, P. Tandon, P. Rawat, R. N. Singh, and A. Singh, "Quantum chemical study of a new reaction pathway for the adenine formation in the interstellar space," *Astron. Astrophys.* **528**, A129 (2011).
- ²³J. Burner, B. J. West, and P. M. Mayer, "What will photo-processing of large, ionized amino-substituted polycyclic aromatic hydrocarbons produce in the interstellar medium?," *J. Phys. Chem. A* **123**, 5027–5034 (2019).
- ²⁴A. Zamir and T. Stein, "Isomerization of hydrogen cyanide and hydrogen isocyanide in a cluster environment: Quantum chemical study," *J. Chem. Phys.* **156**, 054307 (2022).
- ²⁵F. Gardebien and A. Sevin, "Catalytic model reactions for the HCN isomerization. I. Theoretical characterization of some water-catalyzed mechanisms," *J. Phys. Chem. A* **107**, 3925–3934 (2003).
- ²⁶F. Gardebien and A. Sevin, "Catalytic model reactions for the HCN isomerization. II. Theoretical investigation of an anionic pathway," *J. Phys. Chem. A* **107**, 3935–3941 (2003).
- ²⁷S. Nickerson, N. Rangwala, S. W. Colgan, C. DeWitt, X. Huang, K. Acharyya, M. Drozdovskaya, R. C. Fortenberry, E. Herbst, T. J. Lee *et al.*, "The first mid-infrared detection of HNC in the interstellar medium: Probing the extreme environment toward the Orion hot core," *Astrophys. J.* **907**, 51 (2021).
- ²⁸D. B. Rap, A. Simon, K. Steenbakkers, J. G. Schrauwen, B. Redlich, and S. Brünken, "Fingerprinting fragments of fragile interstellar molecules: Dissociation chemistry of pyridine and benzonitrile revealed by infrared spectroscopy and theory," *Faraday Discuss.* (published online, 2023).
- ²⁹H. R. Hrodmarrsson, J. Bouwman, A. G. M. Tielens, and H. Linnartz, "Similarities and dissimilarities in the fragmentation of polycyclic aromatic hydrocarbon cations: A case study involving three dibenzopyrene isomers," *Int. J. Mass Spectrom.* **476**, 116834 (2022).
- ³⁰H. R. Hrodmarrsson, J. Bouwman, A. G. Tielens, and H. Linnartz, "Fragmentation of the PAH cations of isoviolanthrene and dicoronylene: A case made for interstellar cyclo[*n*]carbons as products of universal fragmentation processes," *Int. J. Mass Spectrom.* **485**, 116996 (2023).
- ³¹E. Solano and P. Mayer, "A complete map of the ion chemistry of the naphthalene radical cation? DFT and RRKM modeling of a complex potential energy surface," *J. Chem. Phys.* **143**, 104305 (2015).
- ³²J. Bouwman, A. J. de Haas, and J. Oomens, "Spectroscopic evidence for the formation of pentalene⁺ in the dissociative ionization of naphthalene," *Chem. Commun.* **52**, 2636–2638 (2016).
- ³³K. Ramanathan, A. S. J. Bouwman, L. Avaldi, M. V. Vinitha, P. Bolognesi, R. Richter, and U. R. Kadhane, "Photodissociation of quinoline cation: Mapping the potential energy surface," *J. Chem. Phys.* **157**, 064303 (2022).
- ³⁴H. A. B. Johansson, H. Zettergren, A. I. S. Holm, N. Haag, S. B. Nielsen, J. A. Wyer, M.-B. S. Kirketerp, K. Stochkel, P. Hvelplund, H. T. Schmidt, and H. Cederquist, "Unimolecular dissociation of anthracene and acridine cations: The importance of isomerization barriers for the C_2H_2 loss and HCN loss channels," *J. Chem. Phys.* **135**, 084304 (2011).
- ³⁵A. J. de Haas, J. Oomens, and J. Bouwman, "Facile pentagon formation in the dissociation of polyaromatics," *Phys. Chem. Chem. Phys.* **19**, 2974–2980 (2017).
- ³⁶B. West, C. Joblin, V. Blanchet, A. Bodi, B. Sztáray, and P. M. Mayer, "Dynamics of hydrogen and methyl radical loss from ionized dihydro-polycyclic aromatic hydrocarbons: A tandem mass spectrometry and imaging photoelectron-photoion coincidence (iPEPICO) study of dihydronaphthalene and dihydrophenanthrene," *J. Phys. Chem. A* **118**, 1807–1816 (2014).
- ³⁷P. Castellanos, A. Candian, J. Zhen, H. Linnartz, and A. G. G. M. Tielens, "Photoinduced polycyclic aromatic hydrocarbon dehydrogenation: the competition between H- and H_2 -loss," *Astron. Astrophys.* **616**, A166 (2018).
- ³⁸M. Vinitha, A. M. Nair, K. Ramanathan, and U. R. Kadhane, "Understanding dehydrogenation sequence in fluorene⁺ by multiphoton ionisation–excitation processes," *Int. J. Mass Spectrom.* **471**, 116704 (2022).
- ³⁹M. Rapacioli, A. Simon, C. C. M. Marshall, J. Cuny, D. Kokkin, F. Spiegelman, and C. Joblin, "Cationic methylene-pyrene isomers and isomerization pathways: Finite temperature theoretical studies," *J. Phys. Chem. A* **119**, 12845–12854 (2015).
- ⁴⁰A. Simon, M. Rapacioli, G. Rouaut, G. Trinquier, and F. X. Gadéa, "Dissociation of polycyclic aromatic hydrocarbons: Molecular dynamics studies," *Philos. Trans. R. Soc., A* **375**, 20160195 (2017).
- ⁴¹T. Chen, Y. Luo, and A. Li, "Fragmentation and isomerization of polycyclic aromatic hydrocarbons in the interstellar medium: Coronene as a case study," *Astron. Astrophys.* **633**, A103 (2020).
- ⁴²A. Petrigiani, M. Vala, J. R. Eyler, A. G. G. M. Tielens, G. Berden, A. F. G. van der Meer, B. Redlich, and J. Oomens, "Breakdown products of gaseous polycyclic aromatic hydrocarbons investigated with infrared ion spectroscopy," *Astrophys. J.* **826**, 33 (2016).
- ⁴³P. G. Stoks and A. W. Schwartz, "Basic nitrogen-heterocyclic compounds in the Murchison meteorite," *Geochim. Cosmochim. Acta* **46**, 309–315 (1982).
- ⁴⁴Z. Martins, "The nitrogen heterocycle content of meteorites and their significance for the origin of life," *Life* **8**, 28 (2018).
- ⁴⁵S. J. Clemett, C. R. Maechling, R. N. Zare, P. D. Swan, and R. M. Walker, "Identification of complex aromatic molecules in individual interplanetary dust particles," *Science* **262**, 721–725 (1993).
- ⁴⁶S. A. Sandford, J. Aléon, C. M. O. Alexander, T. Araki, S. Bajt, G. A. Baratta, J. Borg, J. P. Bradley, D. E. Brownlee, J. R. Brucato, M. J. Burchell, H. Busemann, A. Butterworth, S. J. Clemett, G. Cody, L. Colangeli, G. Cooper, L. D'Hendecourt, Z. Djouadi, J. P. Dworkin, G. Ferrini, H. Fleckenstein, G. J. Flynn, I. A. Franchi, M. Fries, M. K. Gilles, D. P. Glavin, M. Gounelle, F. Grossemy, C. Jacobsen, L. P. Keller, A. L. D. Kilcoyne, J. Leitner, G. Matrajt, A. Meibom, V. Mennella, S. Mostefaoui, L. R. Nittler, M. E. Palumbo, D. A. Papanastassiou, F. Robert, A. Rotundi, C. J. Snead, M. K. Spencer, F. J. Stadermann, A. Steele, T. Stephan, P. Tsou, T. Tyliczszak, A. J. Westphal, S. Wirick, B. Wopenka, H. Yabuta, R. N. Zare, and M. E. Zolensky, "Organics captured from comet 81P/Wild2 by the Stardust spacecraft," *Science* **314**, 1720–1724 (2006).
- ⁴⁷M. H. Stockett, J. N. Bull, H. Cederquist, S. Indrajith, M. Ji, J. E. N. Navarrete, H. T. Schmidt, H. Zettergren, and B. Zhu, "Efficient stabilization of cyanonaphthalene by fast radiative cooling and implications for the resilience of small pahas in interstellar clouds," *Nature Commun.* **14**, 395 (2023).
- ⁴⁸P. O'Keeffe, P. Bolognesi, M. Coreno, A. Moise, R. Richter, G. Cautero, L. Stebel, R. Sergio, L. Pravica, Y. Ovcharenko, and L. Avaldi, "A photoelectron velocity map imaging spectrometer for experiments combining synchrotron and laser radiations," *Rev. Sci. Instrum.* **82**, 033109 (2011).
- ⁴⁹B. Dick, "Inverting ion images without Abel inversion: Maximum entropy reconstruction of velocity maps," *Phys. Chem. Chem. Phys.* **16**, 570–580 (2014).
- ⁵⁰M. J. Frisch, G. W. Trucks, H. B. Schlegel, G. E. Scuseria, M. A. Robb, J. R. Cheeseman, G. Scalmani, V. Barone, B. Mennucci, G. A. Petersson *et al.*, *GAUSSIAN09, R. A.*, Gaussian, Inc., Wallingford CT **121**, 150–166 (2009).
- ⁵¹S. Leach, H.-W. Jochims, H. Baumgärtel, and N. Champion, "VUV dissociative photoionization of quinoline in the 7–26 eV photon energy range," *Z. Phys. Chem.* **232**, 845–881 (2018).
- ⁵²J. C. Choe, N. R. Cheong, and S. M. Park, "Unimolecular dissociation of aniline molecular ion: A theoretical study," *Int. J. Mass Spectrom.* **279**, 25–31 (2009).
- ⁵³B. Kaduk, T. Kowalczyk, and T. Van Voorhis, "Constrained density functional theory," *Chem. Rev.* **112**, 321–370 (2012).

- ⁵⁴J. W. L. Lee, M. H. Stockett, E. K. Ashworth, J. E. Navarro Navarrete, E. Gougoula, D. Garg, M. Ji, B. Zhu, S. Indrajith, H. Zettergren, H. T. Schmidt, and J. N. Bull, "Cooling dynamics of energized naphthalene and azulene radical cations," *J. Chem. Phys.* **158**, 174305 (2023).
- ⁵⁵P. Jusko, A. Simon, S. Banhatti, S. Brünken, and C. Joblin, "Direct evidence of the benzylium and tropylium cations as the two long-lived isomers of $C_7H_7^+$," *ChemPhysChem* **19**, 3182–3185 (2018).
- ⁵⁶G. Wenzel, A. Simon, S. Banhatti, P. Jusko, S. Schlemmer, S. Brünken, and C. Joblin, "Infrared spectroscopy of the benzylium-like (and tropylium-like) isomers formed in the $-H$ dissociative ionization of methylated PAHs," *J. Mol. Spectrosc.* **385**, 111620 (2022).
- ⁵⁷S. Banhatti, D. B. Rap, A. Simon, H. Leboucher, G. Wenzel, C. Joblin, B. Redlich, S. Schlemmer, and S. Brünken, "Formation of the acenaphthylene cation as a common C_2H_2 -loss fragment in dissociative ionization of the PAH isomers anthracene and phenanthrene," *Phys. Chem. Chem. Phys.* **24**, 27343–27354 (2022).
- ⁵⁸P. Koskinen, S. Malola, and H. Häkkinen, "Self-passivating edge reconstructions of graphene," *Phys. Rev. Lett.* **101**, 115502 (2008).
- ⁵⁹P. Koskinen, S. Malola, and H. Häkkinen, "Evidence for graphene edges beyond zigzag and armchair," *Phys. Rev. B* **80**, 073401 (2009).
- ⁶⁰A. Chuvilin, J. C. Meyer, G. Algara-Siller, and U. Kaiser, "From graphene constrictions to single carbon chains," *New J. Phys.* **11**, 083019 (2009).
- ⁶¹B. J. West, L. Lesniak, and P. M. Mayer, "Why do large ionized polycyclic aromatic hydrocarbons not lose C_2H_2 ?" *J. Phys. Chem. A* **123**, 3569–3574 (2019).
- ⁶²B. West, B. Lowe, and P. M. Mayer, "Unimolecular dissociation of 1-methylpyrene cations: Why are 1-methylenepyrene cations formed and not a tropylium-containing ion?" *J. Phys. Chem. A* **122**, 4730–4735 (2018).
- ⁶³A. M. Burkhardt, K. Long Kelvin Lee, P. Bryan Changala, C. N. Shingledecker, I. R. Cooke, R. A. Loomis, H. Wei, S. B. Charnley, E. Herbst, M. C. McCarthy, and B. A. McGuire, "Discovery of the pure polycyclic aromatic hydrocarbon indene ($c-C_9H_8$) with GOTHAM observations of TMC-1," *Astrophys. J. Lett.* **913**, L18 (2021).
- ⁶⁴K. O. Johansson, M. P. Head-Gordon, P. E. Schrader, K. R. Wilson, and H. A. Michelsen, "Resonance-stabilized hydrocarbon-radical chain reactions may explain soot inception and growth," *Science* **361**, 997–1000 (2018).
- ⁶⁵L. Zhao, R. I. Kaiser, W. Lu, B. Xu, M. Ahmed, A. N. Morozov, A. M. Mebel, A. H. Howlader, and S. F. Wnuk, "Molecular mass growth through ring expansion in polycyclic aromatic hydrocarbons via radical-radical reactions," *Nat. Commun.* **10**, 3689 (2019).
- ⁶⁶C. He, R. I. Kaiser, W. Lu, M. Ahmed, Y. Reyes, S. F. Wnuk, and A. M. Mebel, "Exotic reaction dynamics in the gas-phase preparation of anthracene ($C_{14}H_{10}$) via spiroaromatic radical transients in the indenyl-cyclopentadienyl radical-radical reaction," *J. Am. Chem. Soc.* **145**, 3084–3091 (2023).
- ⁶⁷J. A. Rundel, C. M. Thomas, P. E. Schrader, K. R. Wilson, K. O. Johansson, R. P. Bambha, and H. A. Michelsen, "Promotion of particle formation by resonance-stabilized radicals during hydrocarbon pyrolysis," *Combust. Flame* **243**, 111942 (2022), A Dedication to Professor Katharina Kohse-Höinghaus.
- ⁶⁸W. D. Watson, "Ion-molecule reactions, molecule formation, and hydrogen-isotope exchange in dense interstellar clouds," *Astrophys. J.* **188**, 35 (1974).
- ⁶⁹M. B. Mendes, H. Buhr, M. H. Berg, M. Froese, M. Grieser, O. Heber, B. Jordon-Thaden, C. Krantz, O. Novotný, S. Novotny, D. A. Orlov, A. Petrigiani, M. L. Rappaport, R. Repnow, D. Schwalm, A. Shornikov, J. Stützel, D. Zajfman, and A. Wolf, "Cold electron reactions producing the energetic isomer of hydrogen cyanide in interstellar clouds," *Astrophys. J.* **746**, L8 (2012).